Carbohydrate Polymers 87 (2012) 943–949

Contents lists available at SciVerse ScienceDirect

Carbohydrate Polymers

journal homepage: www.elsevier.com/locate/carbpol

Short communication

Synthesis, characterization and *in vitro* cytocompatibility studies of chitin nanogels for biomedical applications

N. Sanoj Rejinold[a], Amrita Nair[a], M. Sabitha[a], K.P. Chennazhi[a], H. Tamura[b], S.V. Nair[a], R. Jayakumar[a,*]

[a] *Amrita Centre for Nanosciences and Molecular Medicine, Amrita Institute of Medical Sciences and Research Centre, Amrita Vishwa Vidyapeetham University, Kochi 682041, India*
[b] *Faculty of Chemistry, Materials and Bioengineering, Kansai University, Osaka 564-8680, Japan*

ARTICLE INFO

Article history:
Received 28 June 2011
Received in revised form 29 July 2011
Accepted 17 August 2011
Available online 24 August 2011

Keywords:
Chitin nanogels
Swelling
Drug delivery
Tissue engineering

ABSTRACT

In this work we developed biodegradable chitin nanogels (CNGs) of size 65 nm by controlled regeneration method and characterized. The CNGs showed higher swelling and degradation in acidic pH. The *in vitro* cytocompatibility was analyzed on an array of cell lines and cell uptake studies were done by conjugating CNGs with the rhodamine-123 dye (rhodamine-123–CNGs), which showed retention of nanogels inside the cells. Our preliminary studies reveal that these nanogels could be useful for the delivery of drugs, growth factors for drug delivery and tissue engineering.

1. Introduction

Nanomaterials from chitinous species have a promising future in the biomedical nanotechnology area (Ehrlich et al., 2010; Jayakumar, Deepthy, Manzoor, Nair, & Tamura, 2010a). After significant advances in the fabrication of a wide variety of functional nanomaterials, there has been a growing interest in the field of nanogels (Michalet et al., 2005). Nanogels which are hydrogels confined to nanoscopic dimensions having many attractive properties like size tunability, large surface area, permeability, excellent drug loading capacity, controlled release, responsiveness to environmental stimuli. So they have the potential of becoming an ideal drug delivery system (Jung, Daniel, & Krzysztof, 2007). Chitin is widely used in the biomedical field due to their high biocompatibility and enriched functionalities (Hu et al., 2011; Jayakumar et al., 2010b; Muzzarelli et al., 2007). Compared to synthetic polymer based nanogels, chitin nanogels have an advantage with their functionalities, ligand binding capacity and enhanced biomineralization properties. Chitin is an organo-template for calcium and silica biomineralization in nature (Ehrlich et al., 2008; Ehrlich, 2010a, 2010b). Although significant benefits have been achieved on the relative areas, to the best of our knowledge, there are no studies referring to the chitin nanogels for biomedical applications.

2. Experimental

2.1. Materials

α-Chitin (degree of acetylation – 72.4%) (Koyo chemical Co., Ltd., Japan), $CaCl_2$ and methanol (Qualigens, India) and rhodamine-123 (Sigma–Aldrich). Rhodamine-123 dye was purchased from Biovision, Kochi; DAPI and actin stain (Texas-red phalloidin) were purchased from Sigma–Aldrich. The cell lines were purchased from National Center for Cell Sciences (NCCS), Pune, India.

2.2. Synthesis of nanogels by controlled regeneration chemistry

2.2.1. Synthesis of chitin nanogels (CNGs)

10 mL chitin solution (Tamura, Nagahama, & Tokura, 2006; Tamura, Furuike, Nair, & Jayakumar, 2011), stirred for 1 h, and was treated with methanol till chitin regenerated as gels, which was then washed several times with water till methanol is completely removed from CNGs. This was then centrifuged, followed by higher amplitude (75%) probe sonication for 5 min, and then resuspended in water for further studies. The probe sonication should be done after each centrifugation for 5 min. The whole probe sonication should be done in an enclosed wooden cabin.

2.2.2. Tagging of rhodamine-123 with CNGs (rhodamine-123–CNGs) for cell uptake studies

Rhodamine–CNGs were synthesized by incorporating rhodamine-123 dye after final washing of CNGs. Briefly, 2 mL CNGs were incubated with 40 μL of rhodamine-123 dye for 6 h

* Corresponding author. Tel.: +91 484 2801234; fax: +91 484 2802020.
E-mail addresses: rjayakumar@aims.amriat.edu, jayakumar77@yahoo.com (R. Jayakumar).

0144-8617/$ – see front matter © 2011 Elsevier Ltd. All rights reserved.
doi:10.1016/j.carbpol.2011.08.044

with continuous stirring, finally, the un-bound rhodamine-123 dye were removed by centrifuging the rhodamine-123–CNGs at 5000 rpm for 5 min. The resulting pellet was resuspended in 2 mL millipore water for further studies.

2.3. Biodegradation and swelling studies for the CNGs

The *in vitro* biodegradation of all samples has been studied in acidic, basic and neutral PBS, with and without lysozyme at 37 °C. The biodegradation of the CNGs is compared with control chitin maintained under the same conditions. The weighed lyophilized pellets (W_o) were immersed in three different PBS media, one set containing lysozyme (10^4 U/mL) and the other set devoid of lysozyme and kept for incubation at 37 °C for 45 days. At predetermined time intervals, the samples were taken out and the media was aspirated out completely. The pellets were then vacuum dried for 2–3 h till the moisture content is removed and then weighed (W_t). The degradation was calculated according to the following formula,

$$\text{Degradation}\,(\%) = \frac{W_o - W_t}{W_o} \times 100$$

The swelling was studied at pH 4, 7 and 9, respectively. The lyophilized, weighed CNGs (W_o) were placed in corresponding pH solution for 5 min. The water content from pellet was removed using filter paper and wet weight was recorded (W_w). The swelling ratio was calculated by the following formula.

$$\text{Swelling ratio} = \frac{W_w - W_o}{W_o}$$

2.4. Cell lines and culture protocols

L929 (mouse fibroblast cell line), NIH-3T3 (mouse embryonic fibroblast cell line), KB (oral cancer cell line), VERO cells (kidney epithelial cell line of the African Green Monkey), MCF-7 (human breast cancer cell line) purchased from NCCS, Pune, which were maintained in minimum essential medium (MEM) and PC3 (prostate cancer cell lines, NCCS, Pune) was maintained in Dulbecco's modified Eagles medium (DMEM- F12) supplemented with 10% fetal bovine serum (FBS). The cells were maintained as per the protocol.

2.5. Cell uptake studies by fluorescent microscopy

The cell uptake studies were done according to the previous protocols, (Sanoj Rejinold et al., 2011). The rhodamine-123–CNGs at a concentration of 1 mg/mL were added along with the media in triplicate to the wells and incubated for 2 h for the studies.

2.5.1. Tracking of rhodamine-123–CNGs by DAPI/actin staining

L929, VERO and PC3 cells were used for this study. The cells were grown on cover slips in 24 well plates with a seeding density of 5×10^4/wells for 24 h. The rhodamine-123–CNGs were treated with cells with a concentration of 1 mg/mL. After 24 h incubation with rhodamine-123–CNGs, the cells on the coverslips were washed with PBS after removing the media from the wells, fixed with 5% para formaldehyde for 20 min followed by a PBS wash, thereafter the cells were permeabilized with 0.5% Triton for 5 min, then triton was neutralized with 1% FBS in PBS, washed with PBS, thereafter actin dye was added to the cells according to manufactures protocol. After 1 h incubation with actin stain, 100 μL DAPI (1:15 ratio in PBS) was added in each wells. The stained samples were dried for 24 h. Thereafter, the samples were fixed on slides using DPX as mountant. The samples were analyzed using fluorescent microscopy.

Table 1
Probing parameters for the preparation of CNGs.

	Probing time (min)	Probing amplitude (%)	Particle size measured in DLS (nm)
CNGs (a)	1	25	200 ± 2
CNGs (b)	2	45	150 ± 7
CNGs (c)	3	60	100 ± 5
CNGs (d)	5	75	30 ± 15

2.6. Cytotoxicity studies

For cytotoxicity experiments, L929, NIH-3T3, VERO, MCF7, PC3 and KB cells were seeded on a 96 well plate with a density of 10,000 cells/cm^2. Experiments were done according to the existing protocols (Sanoj Rejinold et al., 2011) for concentrations as 0.1, 0.2, 0.4, 0.6, 0.8 and 1 mg/mL.

2.7. Hemolysis assay

0.2–2 mg/mL of the CNGs have been analyzed here as per the existing protocols. The samples were prepared in 0.9% saline solution (Sanoj Rejinold et al., 2011).

2.8. Analytical characterizations

FT-IR spectra of materials were carried out using KBr tablets (1% (w/w) of product in KBr) with a resolution of 4 cm^{-1} and 100 scans per sample on a Perkin Elmer Spectrum RX1 apparatus. Surface charge and thereby the stability of the same system was obtained by zeta potential measurements (DLS-ZP/Particle Sizer Nicomp^{TM} 380 ZLS). The particle size was measured by dynamic light scattering (DLS-ZP /Particle Sizer Nicomp^{TM} 380 ZLS). The surface morphology of nanogels was analyzed by SEM (JEOLJSM-6490LA) and AFM (JEOL JSPM-5200).

2.9. Statistics

Statistical analysis of the data was performed via one-way analysis of variance (ANOVA) using origin software; a value of $p < 0.05$ was considered significant ($n = 3$).

3. Results and discussions

3.1. Preparation of chitin nanogels (CNGs)

The probing parameters are critical in achieving optimum size as explained in Table 1. Similarly, the centrifugation step allows for complete removal of entire methanol and excess $CaCl_2$. The residual $CaCl_2$ is believed to help in cross-linking of the polymeric chains of chitin. The interplay of other interactions, such as hydrophobic association of major functionalities may also contribute towards the stability of the nanogels.

3.2. Size, morphology and zeta potential of the nanogels

The nanogel carriers in the size range of 10–100 nm will have improved blood circulation time and enhanced extravasation rate into permeable tissues such as tumors. Fig. 1A–C is the DLS, SEM and AFM images, respectively. SEM and AFM analysis confirm that CNGs are nearly spherical in shape with an average diameter of 65 nm. The nanogels showed positive surface of +26.34 mV charge at pH 7.0, which lies in the stable range.

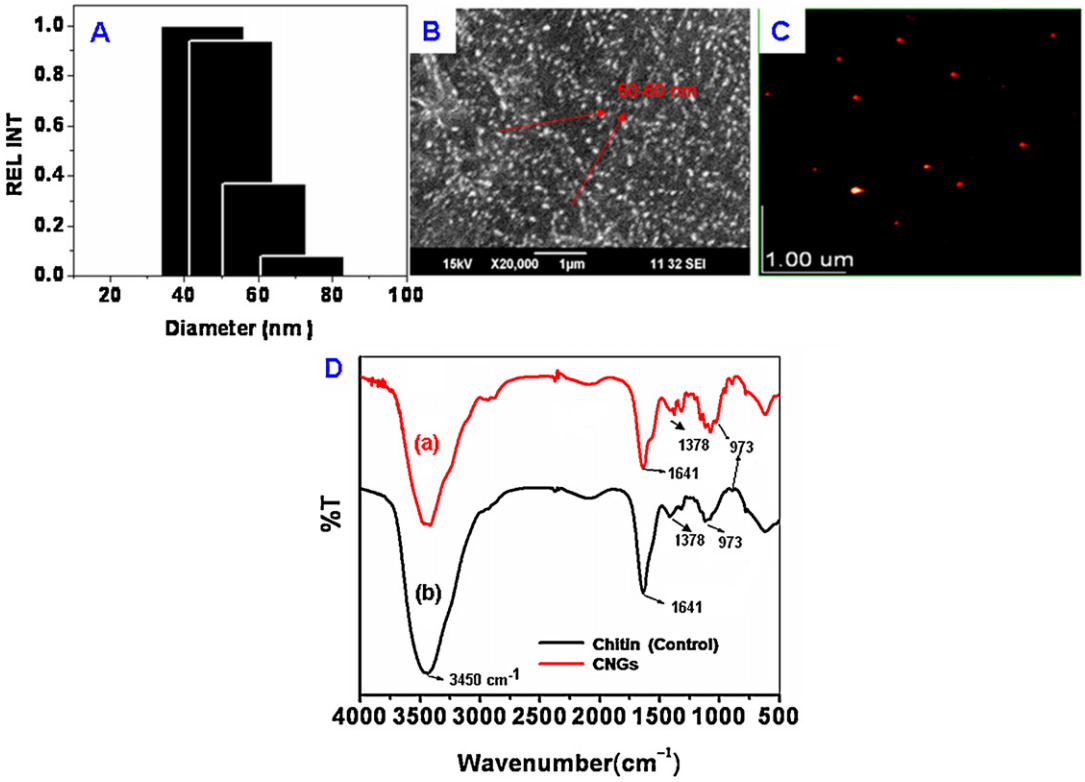

Fig. 1. (A) DLS, (B) SEM, (C) AFM for the CNGs and (D) the FTIR characterization of the chitin control (a) and CNGs (b).

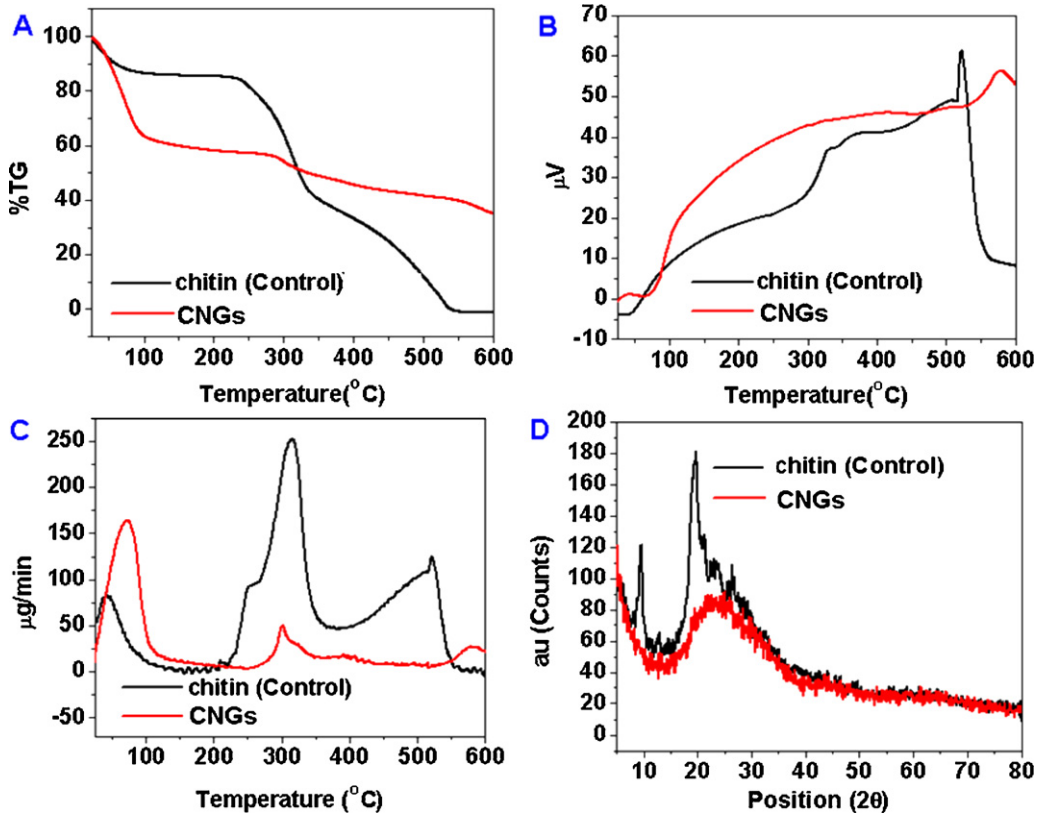

Fig. 2. Thermal analysis by (A) TGA, (B) DTA, (C) DTG and (D) XRD for the CNGs.

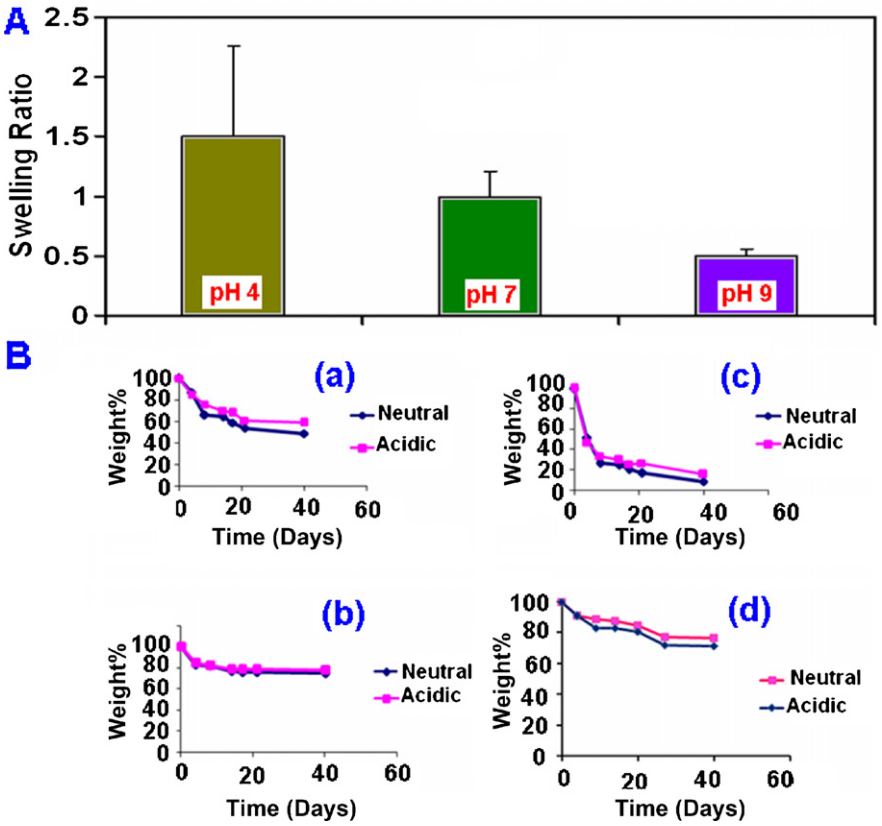

Fig. 3. (A) Swelling studies for the CNGs at different pH 4, 7 and 9; (B) biodegradation studies of (a) CNGs in PBS alone, (b) chitin control in PBS alone, (c) CNGs in PBS and lysozyme, and (d) chitin control in PBS and lysozyme.

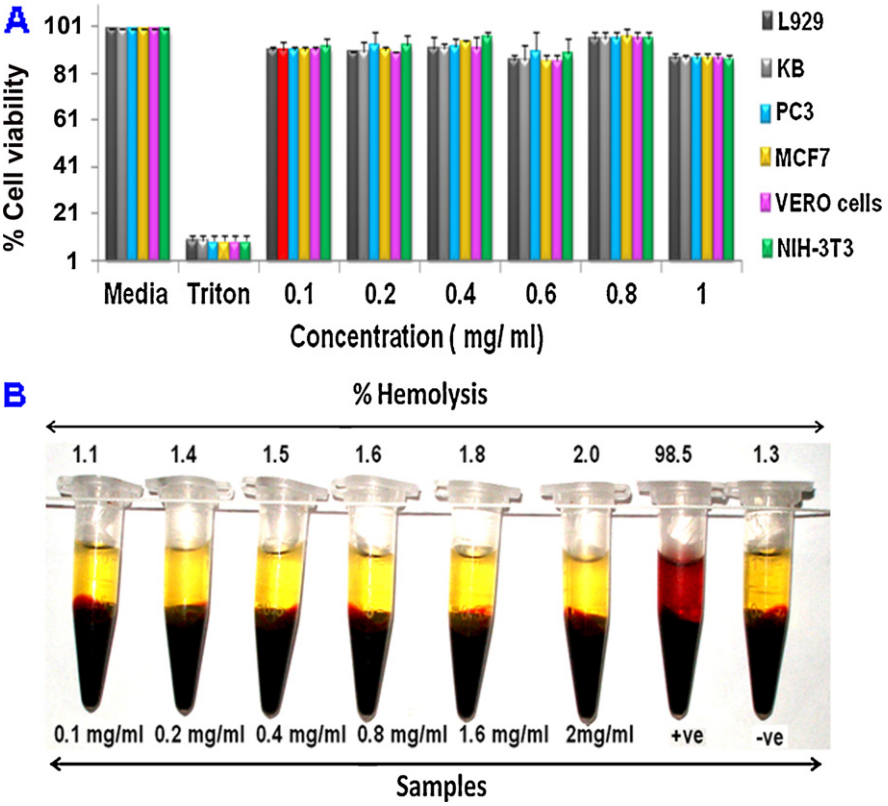

Fig. 4. (A) Cytocompatibility studies for the CNGs on L929; KB; PC3; MCF-7; VERO and NIH-3T3 cell lines. (B) Hemolysis assay for the CNGs with different concentrations from 0.1 to 2 mg/mL in saline.

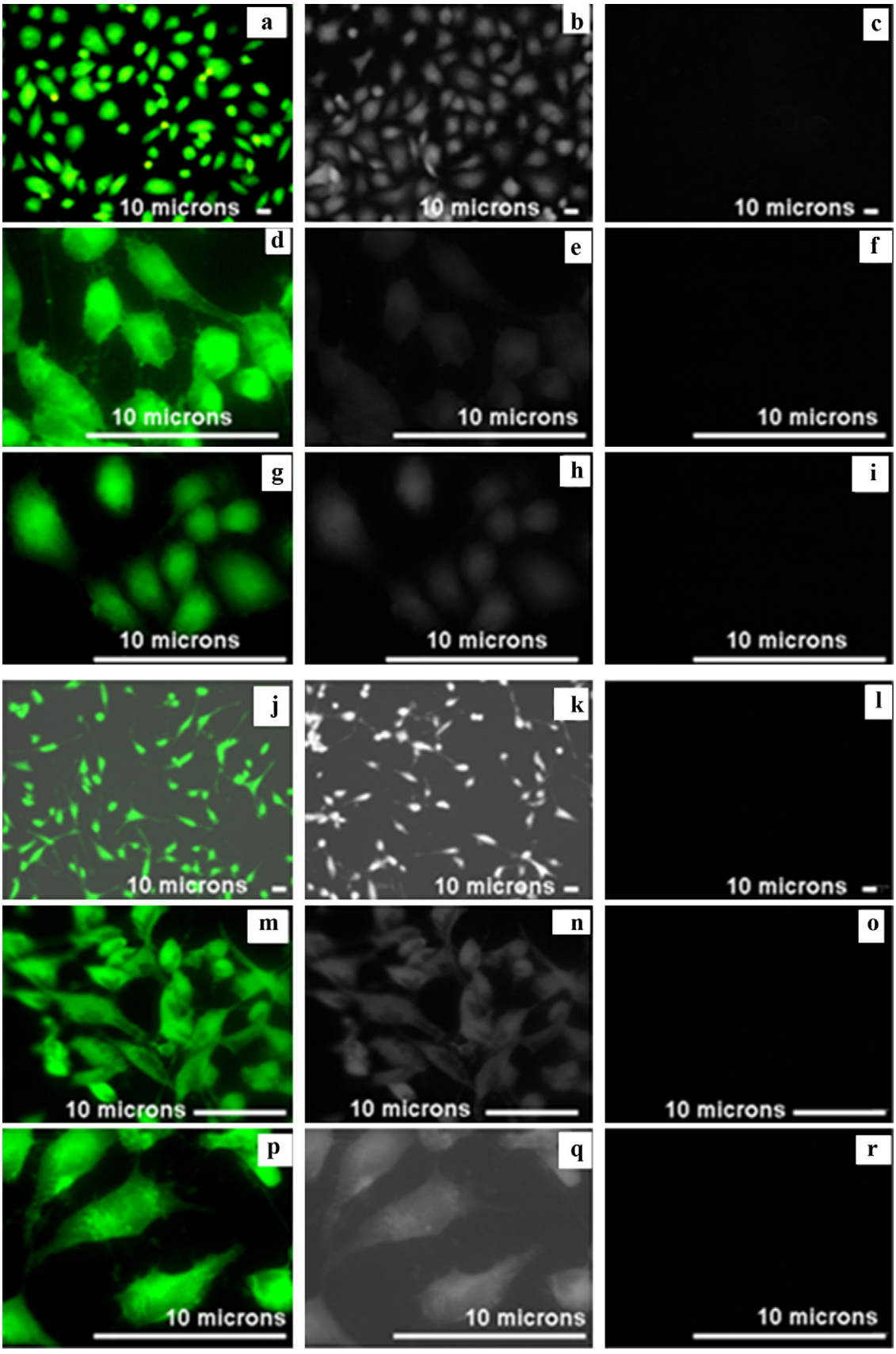

Fig. 5. Cell uptake studies for the CNGs on PC3 (A–I) and VERO cells (J–R) at different magnifications.

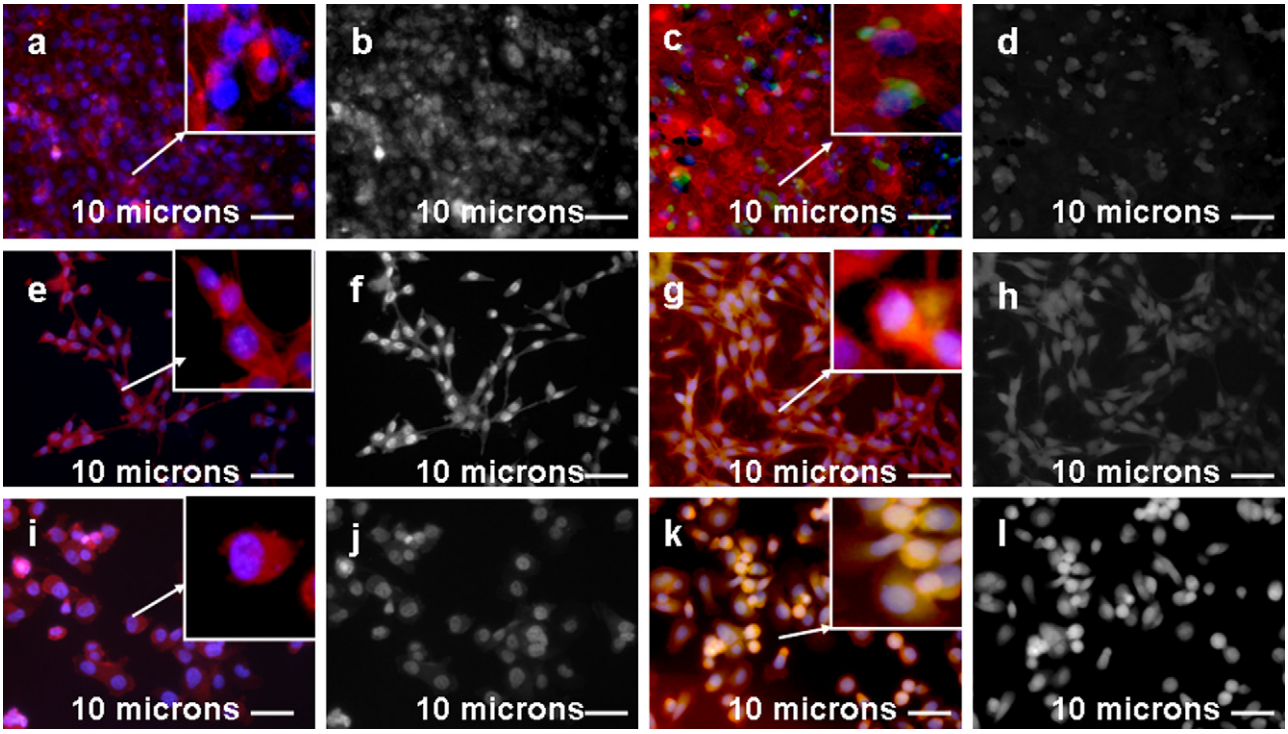

Fig. 6. Cellular trafficking of rhodamine-123–CNGs by DAPI/actin staining on VERO (C and D); L929 (G and H) and PC3 (K and L) cells after 24 h incubation. The control cells have been shown in (A) and (B) (VERO), (E and F) (L929), and (I and J) (PC3). The cells were imaged under fluorescent and bright field view at 20× magnifications in each case.

3.3. Characterization by FTIR, TG/DTA/DTG and XRD

The regenerated material is pure chitin with split transmittance bands at 1660 and 1638 cm^{-1} corresponding to the amide I region and transmittance band at 1560 cm^{-1} corresponding to the amide II region. The existence of 1,4-β-glycosidic bond has been confirmed in both chin and CNGs as shown in the FT-IR spectra (Fig. 1D, a and b). The sharp band at 1378 cm^{-1} has been assigned to $-CH_3$ symmetrical deformation mode of chitin, which is present in CNGs, confirming there is no structural deformation to CNGs from chitin.

Fig. 2 shows the thermograms for CNGs and the chitin (control). In chitins thermogram (Fig. 2), two decomposition steps could be observed, the first occurs in the range of 50–100 °C, and is attributed to water evaporation. The second occurs in the range of 300–400 °C and could be attributed to the degradation of the polysaccharide structure of the molecule. The thermal studies have been compared with existing literatures suggesting an enhanced decomposition rate for the CNGs compared to the control chitin (Stawski, Rabiej, Herczynska, & Draczynski, 2008). The XRD proves improved amorphous nature to the CNGs compared to the control chitin; it could be due to the residual Ca^{2+} inside the CNGs.

3.4. Swelling and biodegradation of chitin nanogels (CNGs)

The swelling study of the chitin nanogel was performed to quantify the amount of swelling that occurs when the nanogel is exposed to different pH 4, 7 and 9. The swelling was higher at acidic pH compared to other pH. This holds well with the hypothesis that the chitin nanogel swells at acidic pH 4 due to the fact that swelling for a polyelectrolyte nanogel takes place at a pH below its pK_a value (6.1) (Raemdonck, Joseph, & De Smedt, 2009) as shown in Fig. 3A.

Biodegradation study was performed on both control chitin and CNGs, and the latter has improved biodegradability, wherein almost 95% (Fig. 3B, c) of the chitin nanogel degraded in the presence of lysozyme. The degradation was a little less without lysozyme and only 60% was degraded (Fig. 3B). This was a great improvement over the control chitin, which underwent only 20% (Fig. 3B, b) degradation in acidic and neutral pH, and not much difference was seen when lysozyme was present. In general, the degradation of chitin can be improved in presence of lysozyme since it can specifically cleave the glycosidic linkages of chitin, thus the N-acetyl-D-glucosamine and the D-glucosamine monomers will be produced as degradation products, which will further enhance the bioactivity of the materials (Sudheesh Kumar et al., 2011). There are no studies referring to the degradation for chitin nanogels.

3.5. Cytocompatibility, cell uptake, cellular trafficking by DAPI/actin staining and hemolysis studies

The nanogels are cytocomaptible for all of the concentrations we studied (Fig. 4A). It is evident from the Fig. 4A that compared to the negative control almost 90% cells are viable in all the six concentrations of CNGs. These results indicated that the prepared CNGs are non-toxic to L929, KB, PC3, MCF7, VERO and NIH-3T3 cells.

Fig. 4B showed that the hemolytic ratio of the sample was far below 5%, the critical safe hemolytic ratio for bio-materials according to ISO/TR 7406, which indicated that all samples from CNGs are hemo-compatible.

The internalization of the rhodamine-123–CNGs was done on PC3 (Fig. 5A–I) and VERO cells (Fig. 5J–R) to prove that they are taken up by these cells without changing the cells' morphology. Additionally, the cellular trafficking of Rhodamoine-123–CNGs was analyzed along with DAPI/actin staining, so that the intracellular localization of the rhodamine-123–CNGs would be easily identified (Fig. 6). The rhodamine-123–CNGs appeared in green/yellowish green whereas the nucleus is blue and the cytoskeletion bright red. (For interpretation of the references to color in this text, the reader is referred to the web version of the article.) These studies clearly confirmed the uptake and cellular localization of rhodamine-123–CNGs and also, even after 24 h incubation period, there are no changes in the cellular morphology, suggesting that

cellular localization of the rhodamine-123–CNGs did not cause any adverse effects.

4. Conclusion

Chitin nanogels have been prepared by regeneration chemistry and characterized by SEM, DLS, FT-IR, TG/DTA/DTG and XRD. Chitin nanogels showed particle size of 65 nm with spherical morphology. The rhodamine-123–CNGs showed good cellular localization in L929, PC3 and VERO cells, without causing any adverse affects. Further, the prepared chitin nanogels have showed enhanced swelling and biodegradability compared to control chitin making it a versatile candidate for various biomedical applications including drug delivery and tissue engineering.

Acknowledgements

The authors would like to acknowledge the Department of Biotechnology, Government of India under a center grant of the Nanoscience and Nanotechnology Initiative program (Ref. no. BT/PR10850/NNT/28/127/2008). One of the authors, N. Sanoj Rejinold would like to acknowledge the Council of Scientific and Industrial Research (CSIR) for the financial support through Senior Research Fellowship (SRF; award no. 9/963 (0017)2K11-EMR). This work is also partly supported by DST, monitored by Dr. C.N.R. Rao.

References

Ehrlich, H. (2010a). Chitin and collagen as universal and alternative templates in biomineralization. *International Geology Review*, *52*, 661–699.

Ehrlich, H. (2010b). *Biological materials of marine origin. Invertebrates*. Springer Verlag., p. 569.

Ehrlich, H., Janussen, D., Simon, P., Bazhenov, V. V., Shapkin, N. P., Erler, C., et al. (2008). Nanostructural organisation of naturally occuring composites: Part II. Silica–chitin-based biocomposite. *Journal of Nanomaterials*, (1). Art. no. 670235, doi:10.1155/2008/670235.

Ehrlich, H., Simon, P., Carrillo-Cabrera, W., Bazhenov, V. V., Botting, J. P., Ilan, M., et al. (2010). Insights into chemistry of biological materials: Newly discovered silica–aragonite–chitin biocomposites in demosponges. *Chemistry of Materials*, *22*, 1462–1471.

Hu, X. W., Tang, Y. F., Wang, Q., Li, Y., Yang, J. H., Du, Y. M., et al. (2011). Rheological behaviour of chitin in NaOH/urea aqueous solution. *Carbohydrate Polymers*, *83*, 1128–1133.

Jayakumar, R., Deepthy, M., Manzoor, K., Nair, S. V., & Tamura, H. (2010). Biomedical applications of chitin and chitosan based nanomaterials – A short review. *Carbohydrate Polymers*, *82*, 227–232.

Jayakumar, R., Prabaharan, M., Nair, S. V., Tokura, S., Tamura, H., & Selvamurugan, N. (2010). Novel carboxymethyl derivatives of chitin and chitosan materials and their biomedical applications. *Progress in Material Science*, *55*, 675–709.

Jung, K. O., Daniel, J. S., & Krzysztof, M. (2007). Synthesis and biodegradation of nanogels as delivery carriers for carbohydrate drugs. *Biomacromolecules*, *8*, 3326–3331.

Michalet, X., Pinaud, F. F., Bentolila, L. A., Tsay, J. M., Dosed, S., & Li, J. J. (2005). Quantum dots for live cells and *in vivo* imaging, diagnostics and beyond. *Science*, *307*, 538–544.

Muzzarelli, R. A. A., Morganti, P., Morganti, G., Palombo, P., Palombo, M., Biagini, G., et al. (2007). Chitin nano fibrils/chitosan glycolate composites as wound medicaments. *Carbohydrate Polymers*, *70*, 274–284.

Raemdonck, K., Joseph, D., & De Smedt, S. (2009). Advanced nanogel engineering for drug delivery. *Soft Matter*, *5*, 707–715.

Sanoj Rejinold, N., Muthunarayanan, M., Sreerekha, P. R., Chennazhi, K. P., Nair, S. V., & Jayakumar, R. (2011). Curcumin-loaded biocompatible thermoresponsive polymeric nanoparticles for cancer drug delivery. *Journal of Colloids and Interface Science*, *360*, 39–51.

Stawski, D., Rabiej, S., Herczynska, L., & Draczynski, J. (2008). Thermogravimetric analysis of chitins of different origin. *Journal of Thermal Analysis and Calorimetry*, *93*, 489–494.

Sudheesh Kumar, P. T., Srinivasan, S., Lakshmanan, V.-K., Tamura, H., Nair, S. V., & Jayakumar, R. (2011). Synthesis, characterization and cytocompatibility studies of α-chitin hydrogel/nano hydroxyapatite composite scaffolds. *Carbohydrate Polymers*, *49*, 20–31.

Tamura, H., Furuike, T., Nair, S. V., & Jayakumar, R. (2011). Biomedical applications of chitin hydrogel membranes and scaffolds. *Carbohydrate Polymers*, *84*, 820–824.

Tamura, H., Nagahama, H., & Tokura, S. (2006). Preparation of hydrogels under mild conditions. *Cellulose*, *13*, 357–364.